IAENG International Journal of Applied Mathematics, 37:1, IJAM_37_1_9

Efficient 2D Linear-Phase IIR Filter Design and Application in Image Filtering

Chi-Un Lei, Chung-Man Cheung, and Ngai Wong *

Abstract—**We present an efficient and novel procedure to design two-dimensional (2D) linear-phase IIR filters with less hardware resource. A 2D linear-phase FIR filter prototype is first designed using semidefinite programming (SDP). The prototype filter is then decomposed into modular structures via Schur decomposition method (SDM). Each section is reduced into IIR structures using a novel digital system identification technique called the Discrete-Time Vector Fitting (VFz). Examples with image processing application show the algorithm exhibits fast convergence and produces low hardware cost and accurate filters.**

Keywords: 2D IIR filter, image processing, digital system identification, vector fitting

1 Introduction

Two-dimensional (2D) filters are widely used in image processing [1], medical imaging [2], face recognition [3] etc. These applications often require high-order filters having accurate magnitude response and linear phase in the passband. For instance, a 63 pixel × 63 pixel kernel filter is used in medical imaging [2]. However, hardware resources are usually restricted due to limited multipliers and memory in ASICs and FPGAs [4]. Therefore, 2D IIR filters are generally used to reduce the hardware cost. However, to date there is no optimal algorithm for 2D IIR filter design in terms of computation and the resultant hardware cost. Direct optimization of an IIR filter gives an excellent accuracy but the computation complexity is high [5]. In the Singular Value Decomposition (SVD) approach, the frequency response of a 2D FIR prototype filter is replaced with parallel sections of 1D cascaded subfilters [6]. The problem is then reduced from a 2D design problem into several 1D design tasks, thus producing less complicated implementation due to parallelization and modularization of filter sections [7]. By neglecting sections associated with small singular values, the decomposed filter can be simplified with only slight error in the filter response [6]. Moreover, subfilters can be reduced by IIR approximation using model order reduction method to further reduce hardware cost. However, this method is complicated when the subfilter sizes and number of sections are large. To this end, we present a novel design flow for designing 2D (near-)linear-phase IIR filters with low computational complexity and hardware cost. First, semidefinite programming (SDP) is used to design a 2D FIR filter prototype, followed by the Schur Decomposition Method (SDM) that decomposes the prototype filter into sections of cascaded 1D FIR subfilters. A novel digital system identification technique, called the Discrete-Time Vector Fitting (VFz), is then used to reduce the 1D FIR subfilters into 1D IIR subfilters. It is shown that VFz gives efficient and accurate IIR approximation over conventional schemes. Practical image processing example demonstrates that the integrated SDP/SDM/VFz design flow produces excellent 2D IIR approximants with good passband phase linearity and low hardware cost.

*The authors are with the Department of Electrical and Electronic Engineering, The University of Hong Kong. Phone: ++852 +2859 1914 Fax: ++852 +2559 8738 Email: {culei, edmondcheung, nwong}@eee.hku.hk

2 Design Methodology

2.1 FIR prototype design via semidefinite programming

The transfer function of a 2D FIR filter of odd order (N_1, N_2) is characterized by

$$H(z_1, z_2) = \sum_{i=0}^{N_1-1} \sum_{j=0}^{N_2-1} h_{ij} z_1^{-i} z_2^{-j} = z_1^T \hat{H} z_2, \qquad (1)$$

where $z_i = \begin{bmatrix} 1 & z_i^{-1} & \ldots & z_i^{-(N_i-1)} \end{bmatrix}^T$ for i = 1 and 2, and $\hat{H} \in R^{N_1 \times N_2}$ is impulse response. This kind of filter with phase linearity becomes octagonal-symmetric [7]. Therefore, $\hat{H}$ can be partitioned as:

$$\hat{H} = \begin{bmatrix} H_{11} & h_{12} & H_{13} \\ h_{21}^T & h_{22} & h_{23}^T \\ H_{31} & h_{32} & H_{33} \end{bmatrix}, \qquad (2)$$

where $H_{11}, H_{13}, H_{31}, H_{33} \in R^{n_1 \times n_2}, h_{12}, h_{32} \in R^{n_1 \times 1}, h_{21}, h_{23} \in R^{n_2} \times 1, h_{22} \in R$ and $n_1 = (N_1-1)/2, n_2 = (N_2-1)/2$. Moreover, the frequency response is given by

$$H(\omega_1, \omega_2) = e^{-j(n_1\omega_1 + n_2\omega_2)} c_1^T(\omega_1) H c_2(\omega_2) \qquad (3)$$

where $c_i(\omega_i) = [\ 1 \quad \cos\omega_i \quad \ldots \quad \cos n_i\omega_i\ ]^T$, for i = 1 and 2, and $H = \begin{bmatrix} h_{22} & 2h_{23}^T \\ 2h_{32} & 4H_{33} \end{bmatrix}$.

(Advance online publication: 15 August 2007)

The design of the prototype FIR filter is a minimax problem of error of H in (ω_1, ω_2) [5]. It can be formulated as

$$\begin{array}{cc} \min & c^T x \\ \text{subject to :} & F(x) \geq 0 \end{array} \tag{4}$$

where $c = \begin{bmatrix} 1 & 0 & \ldots & 0 \end{bmatrix}^T$, and $x = \begin{bmatrix} \delta & h^T \end{bmatrix}^T$, in which $F(x) = diag\left\{\Gamma\left(\omega_1^{(1)}, \omega_2^{(2)}\right), \ldots, \Gamma\left(\omega_1^{(M)}, \omega_2^{(M)}\right)\right\} \geq 0$. Here $\geq$ denotes matrix positive semidefiniteness. A_{dw} is the weighted desired magnitude response. h and c_ω are column vectors by stacking from the first to last columns of H and c_{kn_1+m}, respectively. $c_{kn_1+m}(\omega_1, \omega_2) = \cos(m\omega_1)\cos(k\omega_2)$ for $0 \leq m \leq n_1$, and $0 \leq k \leq n_2$. This is a semidefinite programming (SDP) problem. SDP is an optimization framework wherein a linear or convex objective function is minimized subject to linear matrix inequality (LMI)-type constraints.

2.2 Schur decomposition of 2D FIR filters

The octagonal-symmetric linear phase 2D FIR filters can be decomposed into 1D subfilters by Schur Decomposition Method (SDM) [7]. SDM is superior to SVD in computational complexity by exploitation of filter response symmetry. The idea of SDM is to decompose the 2D transfer function as:

$$H(z_1, z_2) = \sum_{l=1}^{k} F_l(z_1) G_l(z_2), \tag{5}$$

where $F_l(z_1) = \sum_{i=0}^{N_1-1} f_l(i) z_1^{-i}$ and $G_l(z_2) = \sum_{j=0}^{N_2-1} g_l(j) z_2^{-j}$ are the transfer functions of two cascaded 1D subfilters, $f_l(i)$ and $g_l(j)$ are the corresponding impulse responses, and k is the number of parallel sections. k is chosen regarding the tradeoff between computation and approximation accuracy. With the octagonal symmetry, $\hat{H}$ in (2) can be rewritten as

$$\begin{aligned} \hat{H} &= \begin{bmatrix} I_L & 0 \\ \hat{I} & I_M \end{bmatrix} \begin{bmatrix} H_1 & 0 \\ 0 & 0 \end{bmatrix} \begin{bmatrix} I_L & \hat{I}^T \\ 0 & I_M \end{bmatrix} \\ &= \begin{bmatrix} H_1 & H_1\hat{I}^T \\ \hat{I}H_1 & \hat{I}H_1 I^T \end{bmatrix} \end{aligned} \tag{6}$$

where $\hat{I} = \begin{bmatrix} 0 & \cdots & 0 & 1 & 0 \\ 0 & \cdots & 1 & 0 & 0 \\ \vdots & \iddots & & \vdots & \vdots \\ 1 & 0 & \cdots & 0 & 0 \end{bmatrix}$ and $L = n_i + 1$. $H_1 \in R^{L \times L}$ contains all the impulse response information of the 2D FIR filter [7]. H_1 is then decomposed by means of SDM:

$$U^T H_1 U = \sum, \tag{7}$$

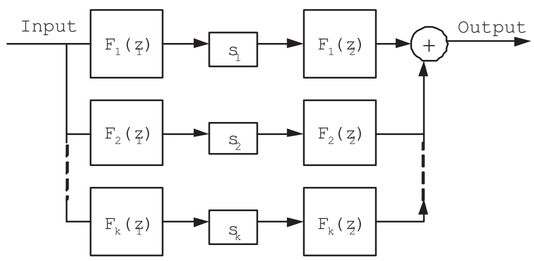

Figure 1: Decomposed FIR prototype filter.

where $U^T U = UU^T = I_L$ and $\sum = diag(\bar{\lambda}_1, \bar{\lambda}_2, ..., \bar{\lambda}_L)$. Retaining the k most significant eigenvalues in $\sum$, namely, $\sum_1 = \sum(1:k, 1:k)$, the approximated 2D FIR filter becomes

$$\tilde{H}_d = W\left|\Sigma_1\right| SW^T = FSG = FSF^T, \tag{8}$$

where $W = \begin{bmatrix} U(:, 1:k) \\ \hat{I}U(:, 1:k) \end{bmatrix}$, $F = W\sqrt{\left|\sum_1\right|} \in R^{N \times k}$, $G = F^T$, and $S = diag(s_1, s_2, ..., s_k)$, in which $s_l = sign\left(\bar{\lambda}_l\right)$, is the sign weight for interconnection between subfilters. Each column of F is an FIR linear phase 1D subfilter with its own frequency response. Therefore, (8) becomes

$$\tilde{H}_d = \sum_{l=1}^{k} F_l s_l F_l^T, \tag{9}$$

$\tilde{H}_d$ preserves phase linearity of the 2D FIR filter. The architecture of the decomposed filter is shown in Fig. 1.

2.3 IIR filter approximation of 1D FIR subfilters

For the sake of hardware savings and consequently power consumption, each of the 1D FIR subfilters (F_1, F_2,..., F_k) is approximated by IIR structures:

$$\sum_{n=0}^{L} h_n z^{-n} = F_l(z) \approx \widehat{f}(z) = \frac{P(z)}{Q(z)} = \frac{\sum_{n=0}^{N} p_n z^{-n}}{\sum_{m=0}^{M} q_m z^{-m}}. \tag{10}$$

where $\widehat{f}(z)$ is the IIR approximant. We aim at locating a set of p_n and q_m with N, M $\ll$ L to form a stable and causal IIR filter with a good approximation subject to constraints like magnitude and phase response, and low algorithmic complexity.

3 Discrete-Time Vector Fitting

Vector Fitting (VF) [8] is a popular technique for fitting continuous-time (s-domain) frequency-dependent vector/matrix with rational function approximations. VF starts with multiplying a scaling function σ(s) to the desired response f(s). The poles on both sides of the equality are set to be equal:

$$\underbrace{\left(\sum_{n=1}^{N}\frac{c_n}{s-\alpha_n}\right)+d+se}_{(\sigma f)(s)} \approx \underbrace{\left(\left(\sum_{n=1}^{N}\frac{\gamma_n}{s-\alpha_n}\right)+1\right)}_{\sigma(s)} f\left(s\right). \tag{11}$$

The basis of partial function ensures well-conditioned arithmetic. The poles (α_n) and residues (γ_n) are either real or exist in complex conjugate pairs. The variables c_n, d, e, and γ_n are solved by evaluating (11) at multiple frequency points. In (11), the set of poles of $(\sigma f)(s)$ and $\sigma(s) f(s)$ are the same. Therefore, the original poles of f(s) cancel the zeros of $\sigma(s)$, which are assigned as the next set of known poles to (11). This iteration process continues until the poles are refined to the exact system poles. In general, it only takes a few iterations. VF is readily applicable to digital domain (z-domain), called Discrete-Time Vector Fitting (VFz), for IIR approximation of FIR filters [9]. In the VFz approach, an initial set of stable poles $\left\{\alpha_n^{(0)}\right\}$ is first assigned to be refined. Analogous to VF, the desired 1D FIR filter response is fitted with a rational function:

$$\underbrace{\left(\sum_{n=1}^{N}\frac{c_n}{z^{-1}-\alpha_n^{(i)}}\right)+d}_{(\sigma f)(z)} \approx \underbrace{\left(\left(\sum_{n=1}^{N}\frac{\gamma_n}{z^{-1}-\alpha_n^{(i)}}\right)+1\right)}_{\sigma(z)} f(z). \tag{12}$$

In digital systems, it is required that $|\alpha_n| > 1$ since stable poles are inside the unit circle. For N_s frequency points at z = z_m $(m = 1, 2, \ldots N_s)$ and $N_s \gg 2N + 1$, (12) is presented in an overdetermined linear equation

$$\left(\sum_{n=1}^{N}\frac{c_n}{z_m^{-1}-\alpha_n^{(i)}}\right)+d-\left(\sum_{n=1}^{N}\frac{\gamma_n f(z_m)}{z_m^{-1}-\alpha_n^{(i)}}\right)\approx f\left(z_m\right), \tag{13}$$

where i is the ith iteration. It can be solved by

$$Ax = b, \tag{14}$$

where the mth row in A, A_m, and entries in the column vector b, b_m, and x are $A_m = \left[\begin{array}{cccccc} \frac{1}{z_m^{-1}-\alpha_1^{(i)}} & \cdots & \frac{1}{z_m^{-1}-\alpha_N^{(i)}} & 1 & \frac{-f(z_m)}{z_m^{-1}-\alpha_1^{(i)}} & \cdots & \frac{-f(z_m)}{z_m^{-1}-\alpha_N^{(i)}}\end{array}\right]$, $x = \left[\begin{array}{ccccccc} c_1 & \ldots & c_N & d & \gamma_1 & \ldots & \gamma_N\end{array}\right]^T$, and $b_m = f\left(z_m\right)$.

To determine the new poles (the reciprocals of zeros of $\sigma(s)$) for next iteration, the poles are computed by the eigenvalues of the following function:

$$\Psi = \begin{bmatrix} \alpha_1^{(i)} & & & \\ & \alpha_2^{(i)} & & \\ & & \ddots & \\ & & & \alpha_N^{(i)} \end{bmatrix} - \begin{bmatrix} 1 \\ 1 \\ \vdots \\ 1 \end{bmatrix} \left[\begin{array}{ccc} \gamma_1 & \ldots & \gamma_N \end{array}\right] \tag{15}$$

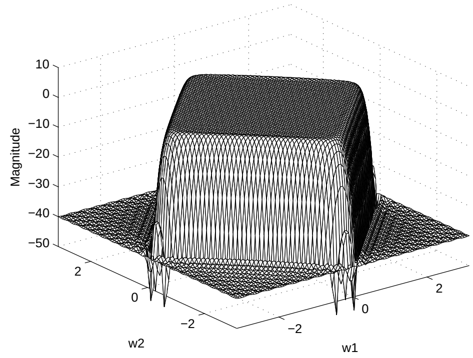

Figure 2: Magnitude response of the 2D prototype lowpass FIR filter by SDP.

To ensure stability, $\left|\alpha_n^{(i+1)}\right|$ must be greater than 1. Unstable poles are relocated by flipping their reciprocals, $1/\alpha_n^{(i+1)}$, into the unit circle. This is possibly done by multiplying both sides of (12) by an allpass filter $\frac{z^{-1}-\alpha_n^{(i+1)}}{1-\overline{\alpha}_n^{(i+1)}z^{-1}}$. Here only the phase is changed. When all the poles converge, $\sigma(z) \approx 1$. It turns out that the IIR denominator part is determined by

$$\tilde{f}(z_m) = \left(\sum_{n=1}^{N}\frac{c_n}{z_m^{-1}-\alpha_n^{(N_T)}}\right)+d \approx f\left(z_m\right). \tag{16}$$

VFz is also extended to handle complex conjugate poles commonly found in digital filters. The accuracy and computational complexity of VFz are dependent of the order of the 1D subfilters, the number of iterations and frequency-sampling points. In short, VFz improves the approximation accuracy successively by using deterministic pole relocation techniques. It is shown by experiments that its accuracy is comparable, if not better, than that of model reduction techniques [10,11], but with much less computational complexity. The saving is even more significant when the number of subfilter sections is large. This result is remarkable. Besides magnitude approximation, VFz simultaneously performs accurate phase approximation, whose linearity is particularly important in image processing.

4 Numerical Example

We would like to verify the performance using two numerical examples. The proposed design methodology is illustrated with a practical lowpass filter example similar to that in [5]. A diamond-shape linear-phase FIR filter with order = (37, 37) is used whose specification is

$$W(\omega_1,\omega_2) = \begin{cases} 0\text{dB}, & \text{for } |\omega_1| + |\omega_2| \leq 0.8\pi \\ -40\text{dB}, & \text{for } |\omega_1| + |\omega_2| > \pi \end{cases} \tag{17}$$

(Advance online publication: 15 August 2007)

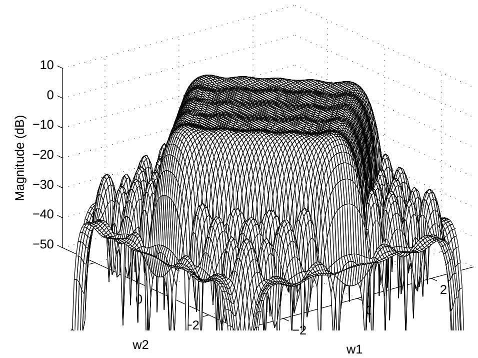

Figure 3: Magnitude response of the approximated 2D lowpass FIR filter after SDM.

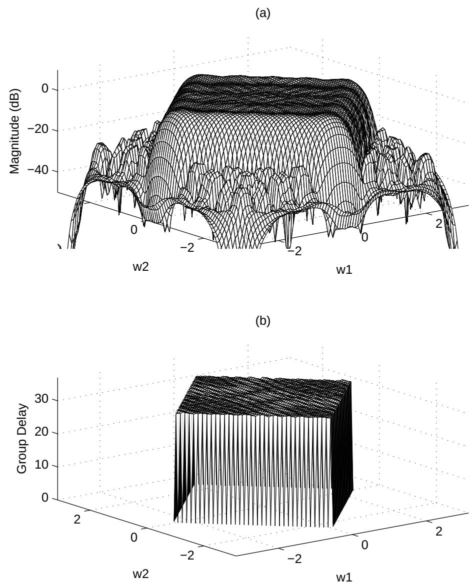

Figure 4: Frequency response of the approximated 2D lowpass IIR filter via VFz: (a) magnitude response and (b) group delay in the passband.

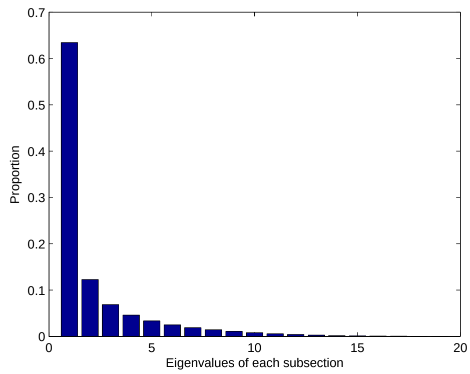

Figure 5: Eigenvalues of the lowpass filter example H_1 of (7) in ratio, which shows the importance of each subsection.

Uniformly distributed grid points of 47×47 are used. The algorithm is coded in Matlab m-script file and run under Matlab 7.2 environment on a 1G RAM 3.4GHz computer. The filter specification is first converted into an SDP problem containing 5651 equations. The prototype filter is decomposed into five sections ($k = 5$) by SDM, which is the most important subsection (sections with the five largest eigenvalues proportion, shown in Fig. 5). Figs. 2 and 3 show the magnitude response of filter after using SDP and SDM, respectively. Each section is then approximated by a 1D IIR subfilter using VFz with orders 19, 20, 19, 20, and 21, respectively. The numerator and denominator in each 1D filter are of the same order. 130 sampling points and 5 iterations are used in VFz. Fig. 4 shows the frequency response of the final 2D IIR filter. The normalized rms errors of the IIR filter approximant are 0.4% and 0.6% in the passband and stopband, respectively. The normalized rms errors between the final design and the ideal design are 4% and 5%, respectively. Furthermore, as seen in the figure, the IIR filter approximant preserves linearity (constant group delay) in the passband and the approximation error is mainly introduced in SDM. The computation time is 507 CPU seconds for FIR prototype filter design (using SDP) and only 1.51 CPU seconds for IIR approximation (using Schur decomposition and VFz approximation). Its advantage in fast computation is therefore demonstrated. Fig. 7 shows that VFz can achieve good approximations for subfilter design. The normalized errors of subfilter approximations are 0.1%, 0.1%, 4%, 4%, and 5%, respectively. Compared to a direct implementation of the original 2D FIR filter, the proposed SDP/SDM/VFz design flow has resulted in a hardware saving (essentially multipliers) of more than 50%. Fig. 8 shows an image noise filtering example.

A bandreject filter example is used in the second example. Bandreject filters are popularly used to remedy images corrupted by additive periodic noise with a known

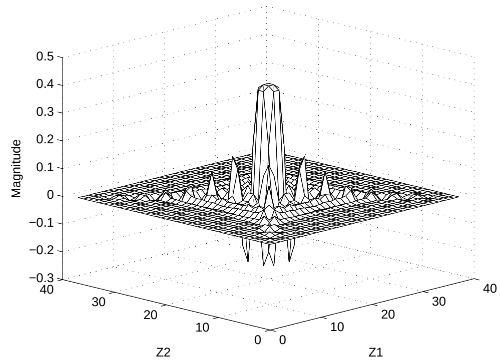

Figure 6: Impulse response of the approximated 2D IIR lowpass filter via VFz.

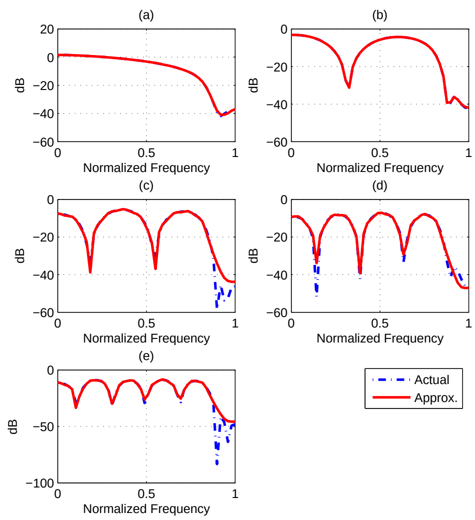

Figure 7: Magnitude response of subfilter approximation using VFz. (a) - (e) are subfilters of sections 1-5 respectively.

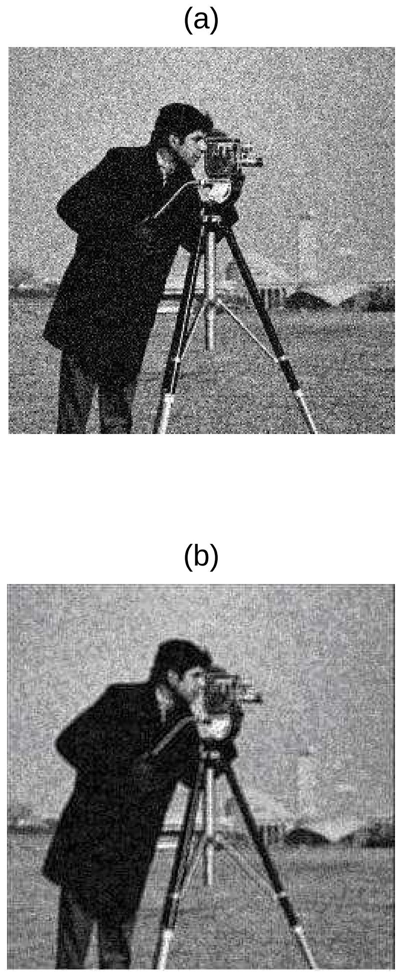

Figure 8: Images in the numerical example. (a) Noise corrupted image. (b) Filtered result using 2D IIR filter.

frequency. A circular-shape linear-phase FIR filter with order = (37, 37) is used whose specification is

$$W(\omega_1,\omega_2)=\begin{cases} 0\text{dB}, & \text{for } 0<\sqrt{\omega_1^2+\omega_2^2}\le 0.5\pi \\ 0\text{dB}, & \text{for } 0.8\pi<\sqrt{\omega_1^2+\omega_2^2}\le \pi \\ -40\text{dB}, & \text{for } 0.6\pi<\sqrt{\omega_1^2+\omega_2^2}<0.7\pi. \end{cases} \tag{18}$$

Uniformly distributed 47× 47 grid points are used. The prototype filter is decomposed into four sections (k = 4) by SDM. Fig. 11 shows the proportion of the eigenvalues. The figure shows that the first few sections have the large rest eigenvalues and contribute most proportion of filter characteristic. Each section is then approximated by a 1D IIR subfilter using VFz with orders 18, 19, 20, and 21, respectively. The numerator and denominator in each 1D filter are of the same order. 100 sampling points and 7 iterations are used in VFz. Figs. 9 and 10 show the frequency response and impulse response of the final 2D IIR filter respectively . As seen in the figure, the IIR filter approximant preserves linearity (therefore, constant group delay) in the passband. Two figures of noise removal are shown in Fig. 12(b) and Fig. 12(c) using 2D FIR prototype filter and 2D IIR filter, respectively. They both show that noise is greatly reduced without much blurring to the original image. The degradation in image quality is small when the 2D FIR prototype filter is replaced with the 2D IIR filter.

The computation time is 528 CPU seconds for FIR prototype filter design (using SDP) and 1.2987 CPU seconds for IIR approximation (using Schur decomposition and VFz approximation). Its advantage in fast 2D IIR approximation is therefore demonstrated. The number of multipliers in the 2D IIR filter is 156, which saves 45.5% multipliers of the original symmetric filter ($37\times 37\div 4=343$). Consequently, it is demonstrated that the proposed IIR filter design flow reduces hardware cost while preserving similar filtering quality when compared to a direct implementation of the original 2D FIR filter.

5 Remarks

1. Besides using SDP, other common and faster design techniques such as the windowing method can be used to design the 2D FIR filter prototype. The SDM/VFz post-processing can then be used to achieve even faster IIR approximation.

2. The most direct approach is to direct decompose the desired frequency response into sections using frequency SVD and then realized each sections by VFz. This can avoid introduced error and relatively time consumed in the 2D FIR prototype filter design. This modification can generate a 2D IIR filter within a few seconds.

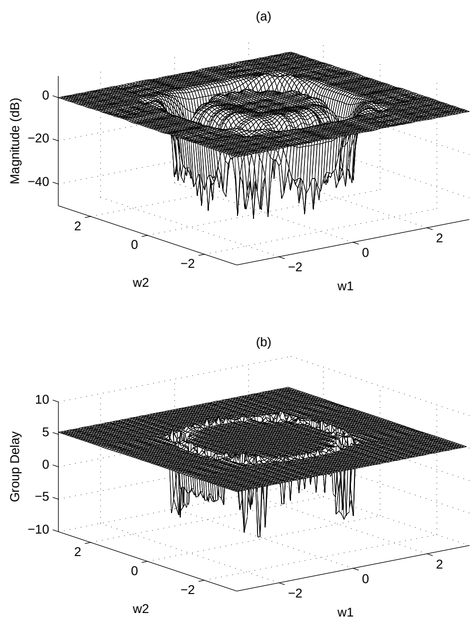

Figure 9: Frequency response of the 2D bandstop IIR filter via the proposed algorithm: (a) magnitude response and (b) group delay in the passband.

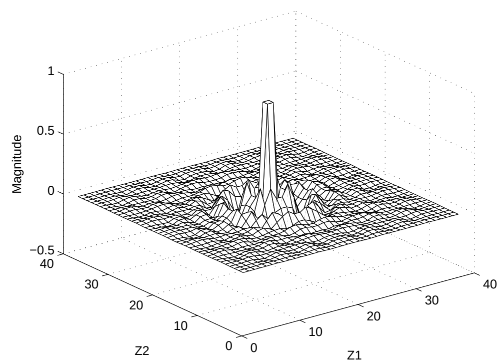

Figure 10: Impulse response of the approximated 2D FIR bandstop filter via VFz.

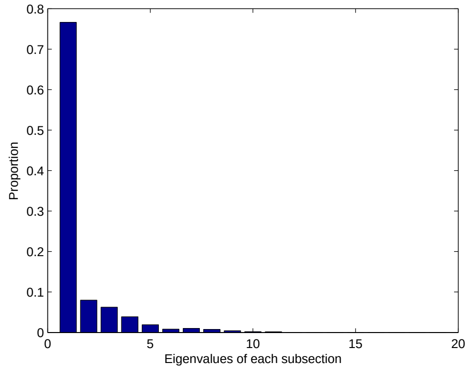

Figure 11: Eigenvalues of the bandstop filter example H_1 of (7) in ratio, which shows the importance of each subsection.

3. In addition to reducing multipliers, the proposed filter structure is also favorable for VLSI implementation. The identical subfilters exhibit regular and modular structures, which lead to reduction in interconnect area and simple floor-planning and layout. Multiplierless filter design techniques are also available for further reducing the hardware cost within the IIR filter structures [12].
4. This paper has extended the Vector Fitting concept to the 2D discrete-time domain. The idea can be further generalized to n-D IIR filter design, which is useful in video processing and medical imaging.
5. Besides the bandreject filter in our example, the proposed algorithm is also applicable to the efficient construction of 2D lowpass, highpass and bandpass filters, with possible applications in image noise removal and edge detection etc.
6. The relationship among error and number of sections and filter orders is still investigated. The investigation objective is to fully integrate Schur decomposition and VFz such that filter can be designed within a controlled error and the lowest hardware cost. As the frequency response in later order is irregular, it is not optimal to use lower order subfilters for later subsections.
7. VFz can be generalized as a frequency masking filter design technique. It is similar as WLS method [13] with novel weighting construction to simplify calculation. Furthermore, VFz can limit the maximum pole radius, which can control the sensitivity of the quantization error.

6 Conclusion

A new 2D IIR filter design flow has been proposed which utilizes the SDP/SDM/VFz integration to efficiently obtain accurate IIR approximants from 2D linear-phase FIR

Figure 12: Images in the numerical example. (a) Noise corrupted image. (b) Filtered result using 2D FIR prototype filter. (c) Filtered result using 2D IIR filter.

filter prototypes. Hardware cost is significantly reduced due to parallel and modular 1D IIR subfilters. Image processing examples have demonstrated that the proposed approach renders high approximation accuracy, low hardware cost, and low computational complexity, and effectively preserves passband phase linearity.

Acknowledgment

This work was supported in part by the Hong Kong Research Grants Council and the University Research Committee of The University of Hong Kong.

References

[1] R. Gonzalex and R. Woods, *Digital Image Processing*, 2nd ed. Upper Saddle River, N.J.: Prentice-Hall, 2001.

[2] R. Kreuger, "Virtex-EM FIR filter for video applications." [Online]. Available: http://direct.xilinx.com/bvdocs/appnotes/xapp241.pdf

[3] S. M. S. Gong and A. Psarrou, *Dynamic Vision: From Images to Face Recognition*, 1st ed. Imperial College Press, 2000.

[4] P. C. C. Bouganis, G. Constantinides, "A novel 2D filter design methodology for heterogeneous devices," in *IEEE FCCM05*, 2005, pp. 13–22.

[5] W. Lu, "A unified approach for the design of 2D digital filters via semidefinite programming," *IEEE Trans. Circuits Syst. I*, vol. 49, no. 6, pp. 814–826, June 2002.

[6] M. A. W.P. Zhu and M. Swamy, "Realization of 2-D linear-phase FIR filters by using the singular-value decomposition," *IEEE Trans. Signal Processing*, vol. 47, no. 5, pp. 1349–1358, Mar. 1999.

[7] R. Aldhaheri, "Design of 2-D linear phase digital filters using schur decomposition and symmetries," vol. 15, no. 1, pp. 65–81.

[8] B. Gustavsen and A. Semlyen, "Rational approximation of frequency domain responses by vector fitting," *IEEE Trans. Power Delivery*, vol. 14, no. 3, pp. 1052–1061, July 1999.

[9] N. Wong and C. Lei, "FIR filter approximation by IIR filters based on discrete-time vector fitting," in *Proc. IEEE Symp. Circuits and Systems*, May 2007, to appear.

[10] B. Beliczynski, I. Kale, and G. D. Cain, "Approximation of FIR by IIR digital filters: an algorithm based on balanced model reduction," *IEEE Trans. Signal Processing*, vol. 40, no. 3, pp. 532–542, Mar. 1992.

[11] H. K. Kwan and A. Jiang, "Recent advances in FIR approximation by IIR digital filters," in *Proc. Int. Conf. Communications, Circuits and Systems*, June 2006, pp. 185–190.

[12] C. Lei and N. Wong, "Multiplierless polynomial-operator-based IIR filters for efficient VLSI implementation," in *IEEE TENCON*, 2006.

[13] W. Lu, S. Pei, and C. Tseng, "A weighted least-squares method for the design of stable 1-D and 2-D IIR digital filters," *IEEE Trans. Signal Processing*, vol. 46, no. 1, pp. 1–10, Jan. 1998.